

**Proceedings of the  
10<sup>th</sup> Australian Space Science Conference  
Brisbane  
27 - 30 September, 2010**



**Australian Space Science Conference Series**

1st Edition

Published in Australia in 2011 by  
National Space Society of Australia Ltd  
GPO Box 7048  
Sydney NSW 2001  
Fax: 61 (02) 9988-0262  
email: [nssa@nssa.com.au](mailto:nssa@nssa.com.au)  
website: <http://www.nssa.com.au>

Copyright © 2011 National Space Society of Australia Ltd

All rights reserved. No part of this publication may be reproduced, stored in a retrieval system or transmitted in any form or by any means, electronic, mechanical, photocopying, recording or otherwise, without prior permission from the publisher.

ISBN 13: 978-0-9775740-4-9

Editors: Wayne Short and Iver Cairns

Distributed on DVD

# Field Strength Measurement of VLF Radio Wave Propagation at 19.8 kHz between Australia and India

\*C. T. More<sup>1</sup>, A. K. Sharma<sup>2</sup> and R. V. Bhonsle<sup>2</sup>  
Kenneth J.W. Lynn<sup>3</sup>

<sup>1</sup> Department of Physics, Miraj Mahavidyalaya Miraj, Dist-Sangli, 416410, India

<sup>2</sup> Department of Physics, Shivaji University, Kolhapur, 416 004, India

<sup>3</sup> Ionospheric Systems Research, 16 Heritage Dr., Noosaville 4566, Australia

\*E-Mail for correspondence: chandrakantmore@yahoo.com

**Summary:** The purpose of this experiment was to study the effect of a solar activity on the field strength of VLF radio wave at 19.8 kHz reflected from D-layer of the Ionosphere. For this, hexagonal loop antenna of 1.5-meter diameter is connected to the VLF receiver tuned to 19.8 kHz. The VLF field strength monitoring system is installed at Khatav, India (16°46' N, 75°53' E). The monitor was used to receive 19.8 kHz transmission by VLF radio station NWC at North West Cape, Western Australia (22°49' S, 114°25' E). The field strength of the VLF radio wave transmitted by the above station via ionosphere was continuously monitored for more than one year at 5 seconds interval. The continuous monitoring of these VLF radio waves from July 30, 2009 to August 31, 2010 clearly shows diurnal and seasonal variation in the field strength. It also shows the effect of solar X-ray flares and annular solar eclipse of January 15, 2010 on the field strength of VLF radio wave propagation. In this paper the analysis and interpretation of the data received is discussed.

**Key words:** VLF radio propagation, diurnal and seasonal variation, solar X-ray flares, annular solar eclipse.

## Introduction

The study of the effects of solar activities like solar flares, sunspots, solar wind particles, coronal mass ejections on the ionosphere of the Earth is very important as they all affect the Earth and its environment. The activities such as UV and X-ray radiation affect VLF (3-30 kHz) radio wave propagation, submarine communication and deep sea navigation. The VLF spectrum has many interesting monitoring possibilities due to its unique characteristics. Field strength monitoring of VLF radio wave transmission via ionosphere of the Earth is an important ground based tool to study solar X-ray flares and also their effects on ionospheric VLF radio wave propagation [1]. The theory of VLF waveguide propagation is at a stage of maturity and thus can be used to interpret a large number of different geophysical phenomena observed on VLF paths [1, 2, 3].

The ionosphere of the Earth is formed due to solar radiation like X-rays, EUV rays as well as cosmic X-radiation. The several ionospheric layers such as D, E and F layers are created with increasing electron densities at different heights [1, 2, 3]. They are also called regions. The D-layer (70-90 kilometers) which is ionized by X-rays of 0.1 to 1 nm, E-layer (100-120 kilometers) ionized by EUV (80-103 nm and X-rays of 1-20 nm) and F-layer forms F1 and

F2 layers during the day ionized by EUV of 20-80 nm (above 120 kilometers ) [4]. Each layer has its own electron density profile with height and their structure changes daily and seasonally under the influence of the sun. The ionospheric behaviors play a role in radio propagation that varies strongly with the frequency. Thus the propagation of VLF radio communications is affected by the ionospheric disturbances At VLF both ground and ionosphere are good electrical conductors and form a spherical earth-ionosphere waveguide and hence the VLF waves transmitted by radio stations propagate by waveguide mode [4, 5, 6]. The VLF radio wave field strength monitoring system (SID Monitor) installed at Khatav (India) captures the 19.8 kHz waves transmitted by VLF radio station NWC Cape North Australia via D-layer in daytime and via E- and/or F-layer in nighttime at the reflection points in the ionosphere.

## Recording and monitoring of VLF signal

The observations reported here were recorded by the VLF field strength monitoring system which is developed by Stanford Solar Center, Stanford University, USA [7] and is situated at Khatav, India (16°46' N, 75°53' E). The receiver has been in stable operation since July 2007, providing well calibrated data from VLF radio station NWC at North West Cape, Western Australia (21°46' S, 114°44' E). With the continuous operation, the received signals reveal regular, diurnal and seasonal field strength variations under quiet and disturbed ionospheric conditions caused by solar activity. Enhancements of signal strength due to increased reflectivity of D-layer caused by even minor solar X-ray flares are very well recorded with this SID monitor at 19.8 kHz.

## The Experimental set up

Fig. 1 shows block diagram of VLF field strength monitoring system which consist of a loop antenna, SID monitor, A/D Converter and Computer.

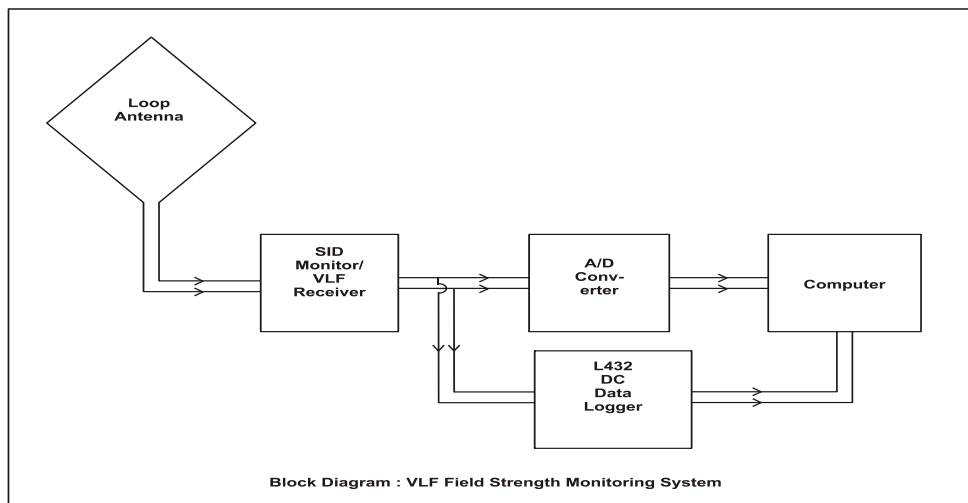


Fig. 1: the block diagram of 19.8 KHz VLF Field Strength Monitoring System

The antenna here used is a hexagonal loop antenna of 1.5 meter diameter, which is made up of 25 turns of 19 gauges super enameled copper wire. The antenna is connected to the receiver by RX-59 coaxial cable and placed at a distance of 45 feet from the receiver. The VLF field strength monitoring system and loop antenna is shown in figure 2. The SID monitor is nothing but VLF amplitude modulation (AM) receiver and it is tuned to NWC Cape North VLF radio station, Australia which is operating at 19.8 kHz. The signal captured by loop antenna is detected, amplified, rectified and the receiver output measures signal strength in DC voltage. The signal is scaled to swing between the two power supply voltages, thus giving the meter as overall 10 volt range (+ or – 5 volt) [9].



(a)

(b)

Fig. 2: 19.8 kHz VLF Field Strength Monitoring System (a) & Hexagonal Loop Antenna (b)

The signal strength data is stored automatically in a computer through A/D converter by using software at 5 seconds interval round the clock.

### Calibration of SID Monitor

Fig.3 shows an experimental arrangement to determine the response of the SID Monitor to the input signal of 19.8 kHz obtained from the function generator. For this purpose, loop antenna was replaced by the function generator. For small input signal, the receiver obeys square law but beyond a certain level of input signal, response of the receiver obeys linear law. The SID Monitor gain or amplification factor is given by the slope of the response curve and is equal to 800 for the input voltages smaller than 4mV. Due to this high gain, the SID Monitor can also receive weak signal.

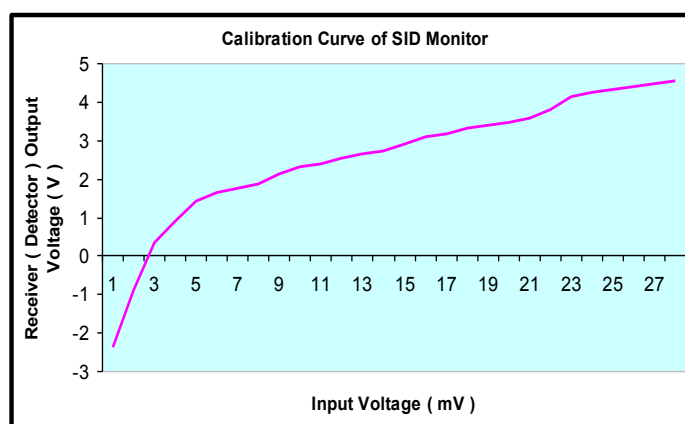


Fig.3: Calibration curve of 19.8 kHz SID Monitor

By using this experimental setup, many C-class and M-class solar X-ray flares are detected in the form of enhancement of VLF field strength. The data recorded shows daily sunrise, sunset effect very clearly and variation of field strength of each day round the clock. The loop antenna is directed towards south east direction so that antenna picks up maximum signal is received.

## Diurnal and seasonal variation

### Diurnal variation

The distance between the NWC 19.8 kHz transmitting station in Australia and Khatav (India) is around 6184 km. Since single-hop VLF radio wave reflection via D-layer does not reach beyond 2000 km [3] an earth-ionosphere waveguide mode of propagation is assumed [4, 5, 6]. The frequency is such that only the first 2 waveguide modes need be considered at night with the first mode probably predominant. Any direct effect of the second mode on this path has yet to be determined.

The word “diurnal” simply means “throughout the day. The diurnal variation of the VLF reflection height is very simple and repetitive. During the day, the reflection height depends almost exclusively on the zenith angle of the sun [3]. This dependence can be seen in fig.4 as a smooth change of field strength in daytime with a maximum at mid-day. At night when the D region has disappeared, the reflection occurs from the very weak night-time E-layer at a height of about 90km. The E region base of the ionosphere at night is less stable than in daytime.

Diurnal variations of VLF signals propagated over long distances (>5 Mm) were first observed by *Yokoyama and Tanimura* [9] in 1933 with diurnal phase variations first reported by Pierce in 1955 and Crombie et al in 1958. During daytime, solar UV and X-rays ionize the neutral atmosphere creating the D, E and F layers. The D layer is created due to ionization of NO by solar L- $\alpha$  (1216Å) radiation. The variation in field strength of 19.8 kHz radio wave on July 30 to 31, 2009 at Khatav, India is shown in fig. 4.

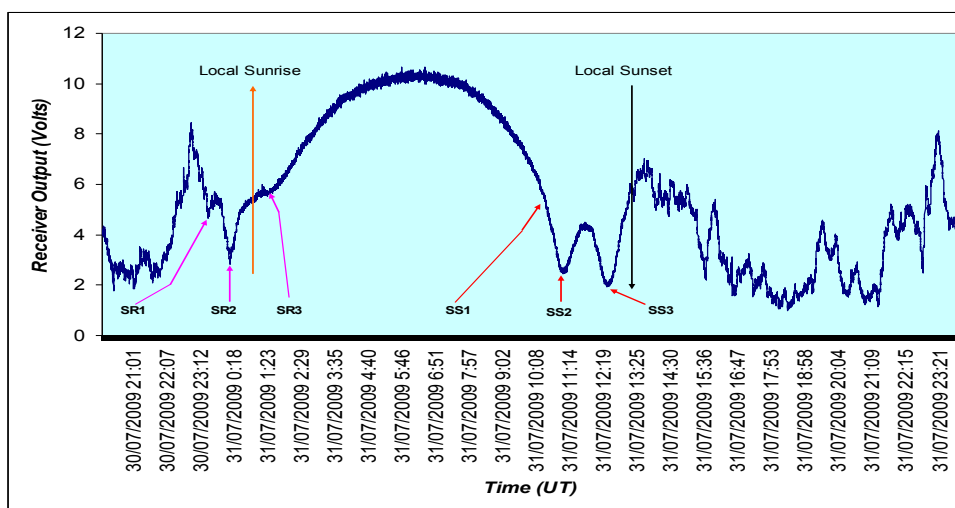


Fig. 4: Typical diurnal variation of NWC signal strength (19.8 kHz) received at Khatav (India) clearly showing sunrise and sunset on July 30 to 31, 2009

The distance between the transmitter (NWC Cape North Australia) and receiver (Khatav, India) is 6184 km. In Fig. 4, the first signal minimum ( $SR_1$ ) observed at the receiver, as the sunrise terminator moves westward over the propagation path, is observed at 23:23 UT (30, July 2009) with a subsequent signal minimum at 00:03 UT ( $SR_2$ ). Following the completion of sunrise over the whole path, an increase in signal strength occurs as a temporary C layer develops [3, 8] when sunlight releases electrons from negative ions built up during the night. A slight kink in signal strength is present ( $SR_3$ ) at 03:04 UT (July 31, 2009) as the D layer begins to build and ultimately swamps the fading C layer, taking over the dominant reflection role. Maximum signal strength occurs in the middle of day when the sun reaches its highest solar zenith angle. Ionizing solar UV on the path is at its maximum at this time and the D region consequently reaches its highest electron density.

Just as two signal minima  $SR_1$  and  $SR_2$  occurred during the path sunrise transition, two signal minima,  $SS_2$  and  $SS_3$  in Fig.4 are observed at 10:19 UT and 10:54 UT (July 31, 2009) during the path sunset transition. The signal minima are produced by modal interference generated at the sunrise and sunset height discontinuities in reflection height as they move along the path [3, 10]. After sunset, the reflection of VLF signals occurs from the E region at a height of around 90 km. This very weak night-time E region is sufficient to reflect VLF radio waves whereas HF radio waves passed through to reflect from the much higher night-time F2 layer. The VLF signal strength is highly variable throughout the night due to the instability of the night-time E layer. The times of local sunrise and sunset are also shown in Fig.4 at 00:28 UT and 13:29 UT respectively.

Somewhat similar “rapid changes of amplitude occur near sunrise and sunset along the path” were observed on a Hawaii-Boulder path (5374 km) on 19.8 kHz [1] with further examples in [10, 3]. The diurnal variation in the signal strength typically repeats day after day.

### **Seasonal variation**

Fig. 5 shows seasonal variation in the field strength of the VLF radio station NWC observed at Khatav (India) for the months from August 2009 to August 2010. The recordings were not done in the months of October 2009 and May 2010 (As the receiving system was under repair in the month of October, 2009 and the transmission from VLF station NWC was not available in the month of May, 2010)

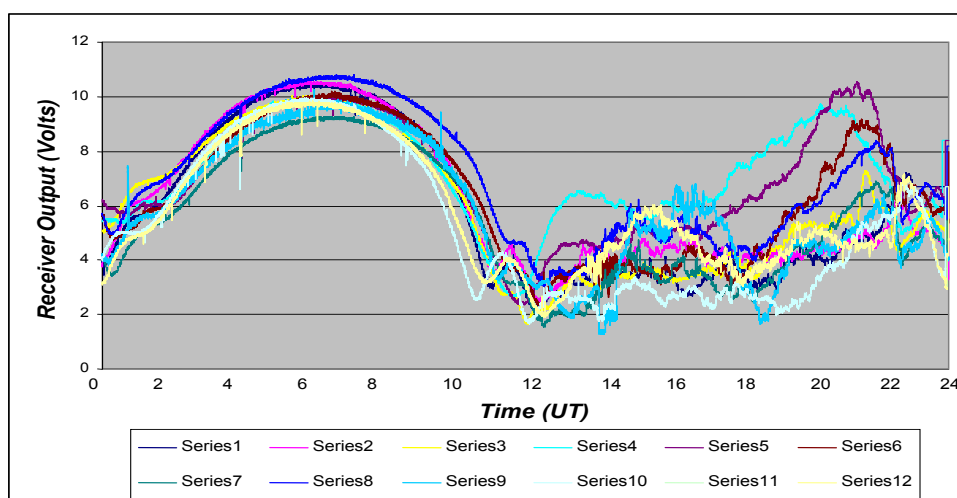


*Fig. 5: Monthly average curves of undisturbed days during the period August 1, 2009 to August*

As explained earlier one can obtain field strength variation at the receiver input by dividing detector output voltage by the amplification factor of the receiver. The monthly average curves of undisturbed days are superimposed in one diagram for easy comparison to bring out seasonal variation.

In table 1 maximum daytime values of detector (receiver) output voltage and field strength at the input of SID Monitor are plotted.

*Table 1- Seasonal variation of maximum daytime field strength of 19.8 kHz transmission (during the period from August 2009 to July 2010) recorded at Khatav (India)*

Month/Year	Maximum daytime detector output(Volts) V	Field strength at the input of SID Monitor mV
August 2009	10.46	1.31
September 2009	10.43	1.32
November 2009	09.92	1.24
December 2009	08.28	1.13
January 2010	08.17	1.12
February 2010	08.76	1.19
March 2010	09.20	1.15
April 2010	09.67	1.21
June 2010	09.82	1.23
July 2010	09.93	1.24

From table 1 it is observed that during the month of August 2009, the signal strength is a maximum and during the month of January 2010, it is a minimum.

### **Effect of solar X-ray flares**

Solar flares which have a strong hard UV and x-rays component have long been known to increase ionization in the D region resulting in a further increase in VLF phase velocity as the reflection height lowers [1, 2, 3, 7, 9]. The VLF signal of 19.8 kHz from NWC is continuously being recorded by a SID monitoring system [7] since April 2007 and shows characteristic variations in diurnal and seasonal field strength. It has been observed that solar flares are huge explosions in the Sun's atmosphere. They appear to instruments as bright flashes in visible light, often followed by a burst of high-energy protons and radiation. Moreover their characteristics can include burst of radio waves, EUV and X-rays [1, 2, 3]. A large solar flare can release a thousand million megatons of energy (more precisely  $10^{28}$  to  $10^{34}$  ergs) in a single explosion. The released energy is transformed into: 1) thermal energy leading to an increased brightness of e.g. the H $\alpha$  and X-ray emission), 2) particle kinetic energy leading to the acceleration of electrons to energies of 10 keV to 1 GeV and ions to energies from a few MeV/nuc to GeV/nuc, 3) mechanical energy leading to several kinds of plasma ejecta. Solar flares sometimes occur together with other signatures of solar activities e.g. prominence eruptions, CME's and interplanetary shock waves. However the exact relationship between these phenomena is not yet completely understood [1]. The most prominent change in the earth-ionosphere waveguide is the diurnal and seasonal variation i.e.

day-to-night (and reverse) change [1]. However, significant modifications of the propagating conditions happen due to severe changes in the lower ionosphere electron density, induced by solar X-ray flares [1, 2, 3]. Although the main source of ionization the Lyman- $\alpha$  emission (1215.67 Å), is enhanced during the flare event, the X-ray emission overwhelms its effect several times, leading to the increase in the D-layer electron density by 1–2 orders of magnitude. Enhanced D-layer density causes the change in the electrical conductivity at the upper waveguide edge along the trace of the VLF signal and consequently, gives rise to the change in all propagating parameters. These changes are clearly detected in the form of VLF field strength variation. Although flare effects on the VLF signal are always well recognizable, they can vary substantially along different signal traces. The theory of VLF propagation through the earth-ionosphere waveguide, at regular (quiet) ionospheric conditions, is well established [5, 6]. When solar flares occur, sudden energy bursts in the X-ray domain appear most distinctly impressed on the VLF signal, by amplitude with an abrupt increase, followed by the subsequent signal recovery within time intervals (typically less than an hour), which correspond to flare duration [8]. Over 50 flare events were detected during the period of July 1, 2009 to July 30, 2010. We relate the VLF signal variations measured by the VLF field strength monitoring system to the solar X-ray irradiance, as monitored by the GOES 12 satellite. Fig. 6 gives representative example of flare-induced field strength variations, measured for the NWC signal, on the active day of December 22, 2009. This sudden field strength variation is related to the C-5 Class solar x-ray flare detected by GOES X-ray satellite which is shown in fig 8 by the mark 1 in blue colour.

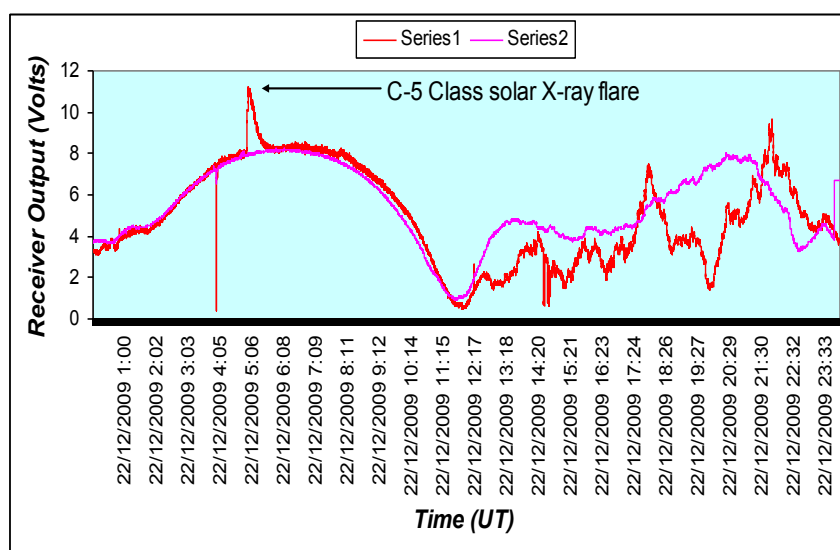


*Figure 6: Diurnal field strength variation of NWC Cape North Station. Series 1- red colour curve corresponds to C-5 Class Solar X-ray Flares occurred on December 22, 2009. Series 2- pink colour curve shows the average diurnal field strength variation for the month of December 2009.*

Fig. 6 shows the unperturbed average plot of field strength of the month of December 2009 is overlapped with the plot of disturbed day December 22, 2009. This perturbation is observed due to C-class solar X-ray flare. The correspondence between the X-ray flare events detected by GOES 12 satellite enhancement is remarkable; moreover, the field strength response to the flare is clearly present. Fig. 7 gives another example of flare-induced field strength variations, measured for the NWC signal, on the active day of December 23, 2009. This sudden field



strength variation is related to the C-5 Class solar x-ray flare detected by GOES X-ray satellite which is shown in fig 8 by the mark 2 in blue colour.

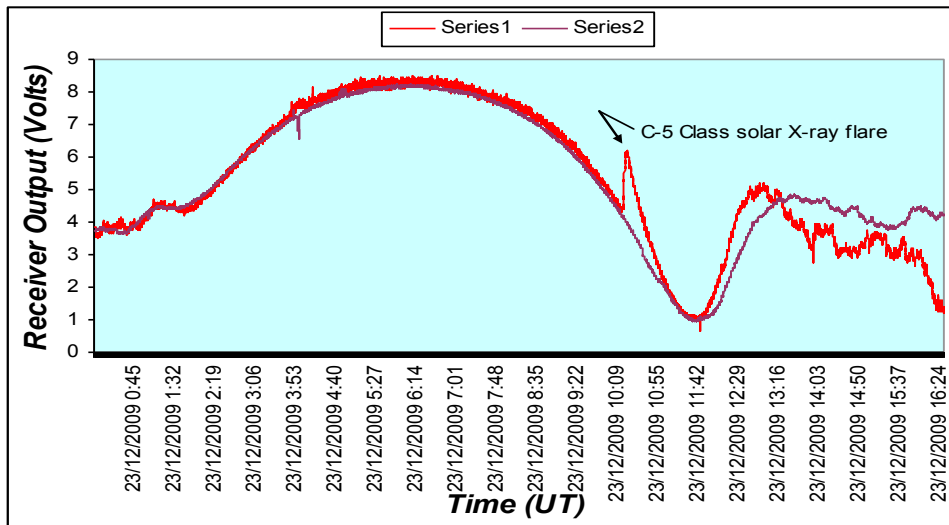


Figure 7: C-5 Class Solar X-ray Flares occurred on December 23, 2009

The Fig. 8 shows the solar X-ray irradiance as monitored by GOES 12, from December 22 to 24, 2009 (UT), indicating a sequence of flares of class B and class C. The features of enhanced

X-ray irradiance have a distinct impact upon VLF field strength characteristic, which display different patterns peculiar to the NWC path, throughout a single active day.

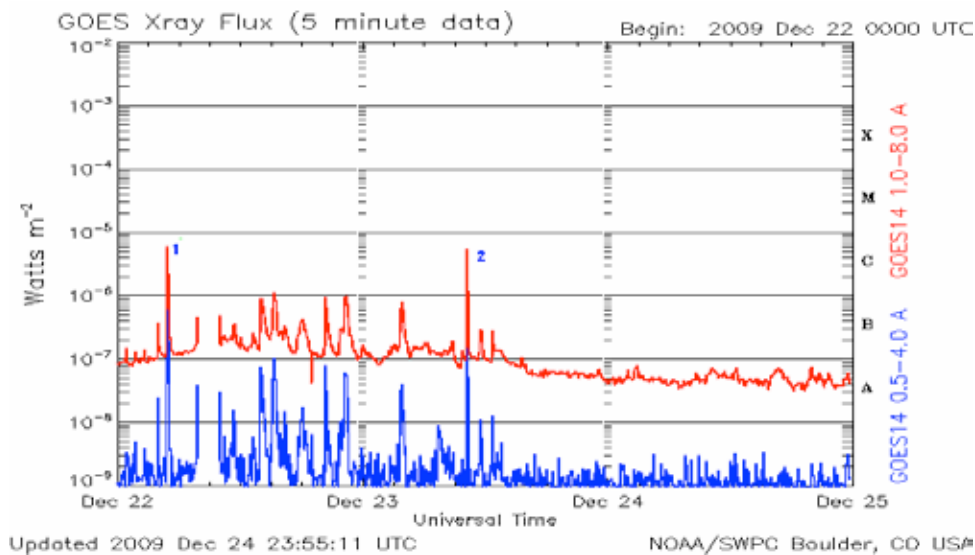


Fig. 8: GOES X-ray flux plot on December 22 to 24, 2009 Figure 9: Optical photo of sun on Dec. 23, 2009

During a solar flare, VLF waves travel at a reduced incidence angle to the earth and ionosphere as the D region expands downward thus narrowing the waveguide. The signal

strength usually increases because the wave does not lose energy as it reflects from bottom of the D-layer. However, the VLF signal strength during flare can sometimes decrease. As soon as X-ray flares end, the sudden ionospheric disturbance (SID) starts to decay and the electron density in the D-layer returns to normal as a result of attachment and /or recombination processes. The VLF field strength monitoring system has also recorded many B-class solar X-ray flare events along with those of M and X-class. The plot of signal strength against time recorded on December 22, 2009 can be compared with the GOES satellite data graphs available at <http://www.swpc.noaa.gov/ftpdir/plots/x-ray>. We can also confirm the H-alpha line images of the sun on the same day and correlate the event and X-ray flare. We can also do correlation study between the sunspots and solar X-ray flares.

## Multiflare analysis

For the analysis of VLF data, a series of flares were selected that occurred on January 20, 2010 and they are presented, along with the average VLF field strength measurements, in figure 9. The reasons for this choice are as follows: 1) the flare intensity (ranging from class C to M) is characteristic for the majority of the flares that have been VLF recorded at Khatav (India) on this active day. (2) many SIDs in the form of signal enhancements overlapping in occurrence due to multiple solar X-ray flares have been recorded on this day from sunrise to sunset.

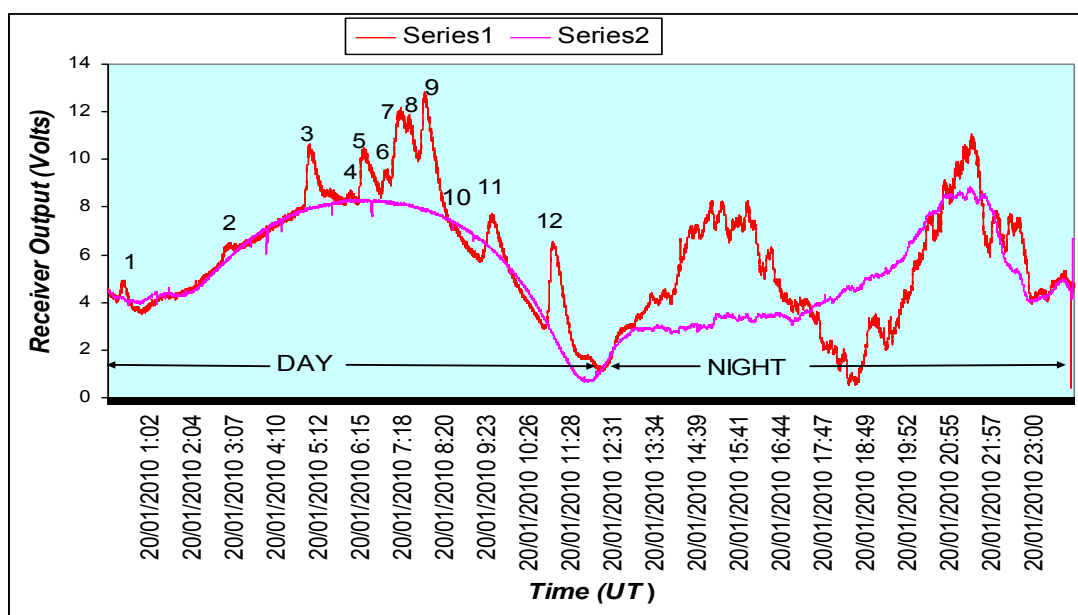


*Fig. 9: Multiflare occurrence on active day of January 20, 2010*

Fig. 10 shows the GOES 12 satellite X-ray plot on active day of January 19, and 20, 2010. It is observed that solar X-ray flare events started to occur from January 18, 2010 and these solar activity ends on January 21, 2010. It is also observed that many M-class and C-class solar X-ray flares have been occurred during this period.

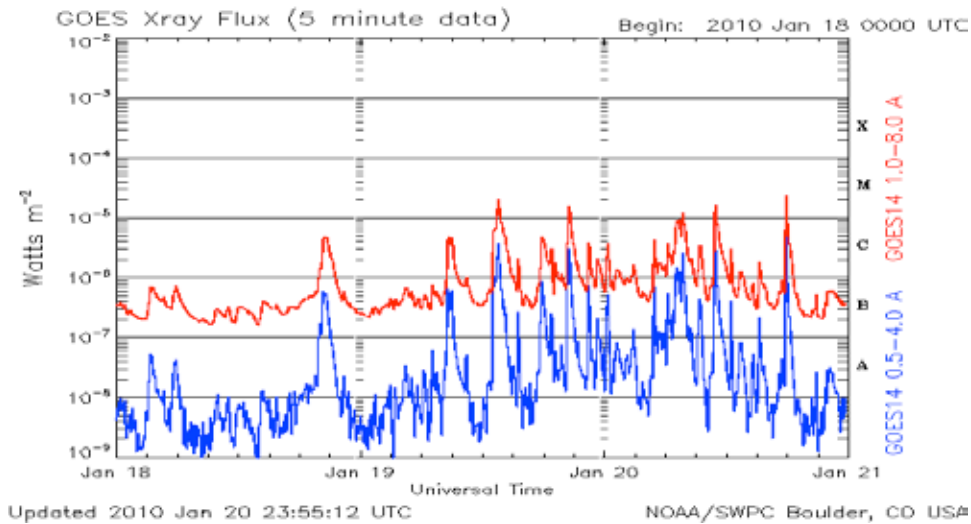


Fig.10: GOES 12 satellite X-ray plot on active day of January 19, and 20, 2010

The characteristics of the flare events are given in Table 2: The first column identifies the flare number the second column lists the time at which the characteristic feature of the field strength variation (minimum/maximum) is detected. The third column shows the duration of events.

Next column four shows the output voltage of detector when flare occurred and column five shows the average detector output voltage for the month of January 2010. The column six shows variation  $\partial V$  in detector output. The column seven shows the Class of flare and the last column shows the Flare Intensity ( $W/m^2$ ) as the data recorded by satellite GOES 12.

Table 2: Measured field strength variation at different stages of flare occurrence and at different angle of elevation and intensity of X-ray flares

Solar Elevation Angle	Flare No.	Flare Time (UT)			Duration (Minutes)	$V_f$ (Volts)	$V_q$ (Volts)	$\partial V$ (Volts)	Class of flare	Flare Intensity ( $W/m^2$ ) as satellite GOES 12 data
		Start	Max	End						
21°	1	00.13	00.23	00.30	17	4.82	4.11	0.72	C4	$4 \times 10^{-6}$
58°	2	02.49	02.58	03.13	24	6.44	3.81	2.63	C1	$1 \times 10^{-6}$
73°	3	04.50	04.58	05.22	32	10.47	8.01	2.46	C1	$1 \times 10^{-6}$
77°	4	05.51	06.00	06.11	20	8.54	8.27	0.26	C6	$6 \times 10^{-6}$
72°	5	06.13	06.20	06.46	33	10.25	8.24	2.02	C5	$5 \times 10^{-6}$
64°	6	06.46	06.53	07.00	14	9.57	8.21	1.36	C7	$7 \times 10^{-6}$
61°	7	07.00	07.16	07.23	23	12.17	8.14	4.03	C8	$8 \times 10^{-6}$
56°	8	07.23	07.28	07.41	18	11.72	8.05	3.67	C9	$9 \times 10^{-6}$
52°	9	07.41	07.51	08.33	52	12.62	7.79	4.83	M1	$1 \times 10^{-5}$
39°	10	08.33	08.39	08.46	13	7.31	7.09	0.22	C2	$2 \times 10^{-6}$
30°	11	09.15	09.30	10.01	46	7.55	5.82	1.73	C5	$5 \times 10^{-6}$
8°	12	10.50	11.03	11.38	48	6.38	1.94	4.45	M2	$2 \times 10^{-5}$

### Determination of field strength variation $\partial V$ due to X-ray flares

The field strength variation  $\partial V$  is determined from the VLF field strength measurements on the quiet day  $V_q$ , and that due to X-ray flare  $V_f$  is given by

$$\{\partial V\} = \{V_f - V_q\} \quad (1)$$

It can be seen from Table 2 that the smallest enhancement in field strength (as measured by the detector output) is 0.214 volts and largest one is 4.828 volts. However, amount of field strength enhancement depends upon the intensity of X-ray flux and solar elevation angle. If the detector output voltage is divided by amplification factor of the receiver, one can get field strength variation at the receiver input terminal. Thus it is clear that our SID Monitor (VLF Field Strength Monitoring System) is very sensitive and can detect even very minor solar X-ray flares recorded by GOES 12 Satellite.

### Effect of annular solar eclipse of January 15, 2010

The solar eclipse of January 15, 2010 was an annular eclipse of the Sun with a magnitude of 0.9190. This was the longest duration annular solar eclipse of the millennium with a maximum duration of 11 minutes and 7.7 seconds. It was visible as a partial eclipse in much of Africa, Eastern Europe, Middle East and Asia. It was seen as annular within a narrow stretch of 300 km width across Central Africa, Maldives, South Kerala (India), South Tamil Nadu (India), North Sri Lanka, parts of Burma and parts of China. The eclipse started at the Central African Republic, traverses Cameroon, Congo and Uganda passes through Nairobi, Kenya, and enters the Indian Ocean and reaches greatest eclipse. It was the longest on land with 10.8 minutes of viewing.

In Fig. 11, the red track shows the path of annular solar eclipse of January 15, 2010. The different ellipses and circles shown in this figure are the shadows of moon at different regions on the surface of the Earth along the eclipse path.

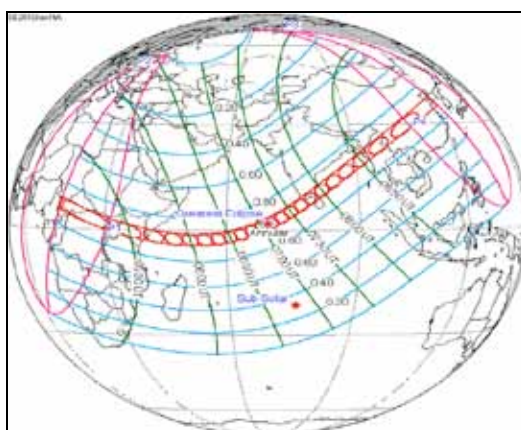


*Fig. 11: Path of annular solar eclipse of January 15, 2010*

On January 15, 2010, the field strength monitoring system recorded the VLF signal of NWC. The eclipse path and path of VLF waves crossed with each other over the Indian Ocean. Fig. 12 shows field strength variation on three days during the annular solar eclipse of January 15, 2010 (pink line- January 14, green line – January, 16 and red line - January 15, 2010). The

departure of eclipse day field strength from the diurnal variation of the month of January, 2010 can be seen from the figure 12 in which decrease in the field strength can be attributed to decrease of flux (Lyman  $\alpha$ -1216 Å).

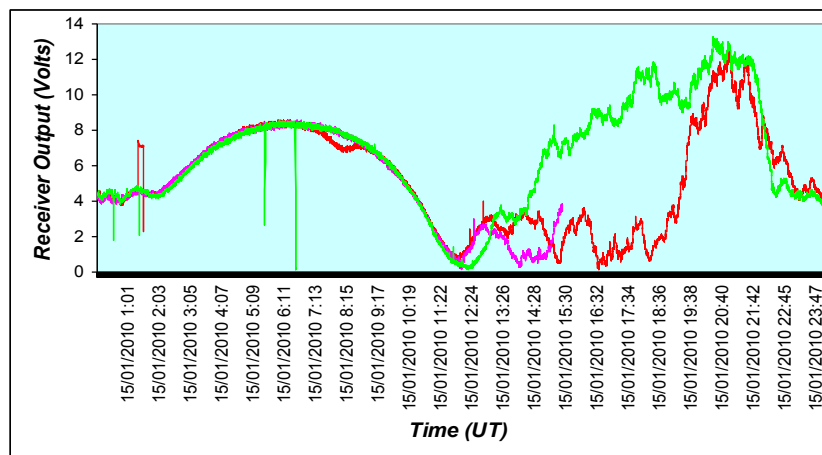


*Fig. 12: Field strength variation on three days during the annular solar eclipse of January 15, 2010 (pink line- January 14, green line – January, 16 and red line - January 15, 2010)*

On January 15, 2010 the field strength of NWC started to decrease its value as the moon shadow started to fall on the VLF radio wave path from NWC Australia to Khatav (India) over the Indian Ocean at 07:15 UT. The maximum dip in field strength is observed at 08:15 UT. After this dip the field strength again started to increase and it recovered its quiet day value at 09:00 UT. So the total time of effect of annular solar eclipse on VLF path from NWC to Khatav (India) is 1 hour and 15 minutes.

## Conclusion

### 1. Diurnal and seasonal variation

A VLF field strength monitoring system is very useful for the study of solar activity including solar X-ray flares, sunspots, solar wind particles and coronal mass ejections. It is also useful to study the lower parts of the quiet ionosphere as observed on the field strength of VLF signals from distant VLF radio stations. The amplitude of the NWC signal as recorded at the Khatav site (India) varies only slightly from day to day during quiet days of minimum solar disturbance (from local sunrise to local sunset). The effect of mode conversion during sunrise and sunset on the field strength of 19.8 kHz NWC transmission observed at Khatav (India) is also repetitive and has yet to be studied in detail. The pattern of diurnal and seasonal variation in field strength has been described.

### 2. Effect of solar x-ray flares

VLF amplitude of the NWC Cape North 19.8 kHz transmitter recorded by the field strength monitoring system at Khatav (India) have been analyzed for about 50 solar X-ray flare events, during the period July 2009 to July 2010. The measured field strength variation and their characteristic features, specific for the NWC path, which is almost over Indian Ocean, have been related to the solar flare intensities, as monitored by the GOES-12 satellite. The results arrived at allow for the classification of solar X-ray flares by their effect on the lower ionosphere and indicate the possible mechanisms of VLF propagation in perturbed conditions: 1. Low C-class flares cause a small increase of field strength up to a single maximum appearing with a time delay of a few minutes after peak X-ray irradiance (flare

events C3 and C2). A likely explanation for the increase in field strength can be found in the field strength enhancement as the signal penetrates the D-layer undergoing ionization redistribution. Along with the electron density increase, the upper boundary of the waveguide drifts slightly downwards to lower heights.

### **3. Effect of annular solar eclipse**

The variation in the field strength of the NWC transmitter was observed during the annular solar eclipse of January 15, 2010, which was attributed to decrease of UV flux (Lyman  $\alpha$ -1216 Å) thereby decreasing reflectivity of D-layer).

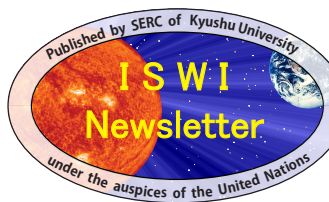
## **Acknowledgements**

The supports and encouragements from Prof. Dr. Deborah Scherer of Stanford University USA (for providing SID Monitors tuned at 19.8 and 24 KHz , data logger, software etc) as well as co-operation and encouragements from Prof. Sharad Patil , chairman of Yashawant Shikshan Sanstha Sangli (India) Prof. Dr. J. B. Chaugule (Former Principal ) and Prof. Smt. Bharamgude S.S.(Principal) of Miraj Mahavidyalaya Miraj (India) are gratefully acknowledged. The authors would like to thank Prof. Dr. S. D. Khambe of Miraj Mahavidyalaya Miraj (India) for significant help in preparation of this paper.

## **References**

1. Davies K. “*Ionospheric Radio Propagation*”, NB5 Monograph 80, 1975.
2. Barr R, I., D. L. Jones, C. J. Rodger, “ELF and VLF Radio Waves”, *J. of Atmos. and Solar- Terr. Phys.*, 62, 1689 (2000).
3. Lynn, K. J. W., “VLF Waveguide Propagation: The Basics”, *PROPAGATION EFFECTS OF VERY LOW FREQUENCY RADIO WAVES*: Proceedings of the 1st International Conference on Science with Very Low Frequency Radio Waves: Theory and Observations. AIP Conference Proceedings, Volume 1286, pp. 3-41, DOI: [10.1063/1.3512893](https://doi.org/10.1063/1.3512893), 2010.]
4. Budden K.G., “*The Waveguide Mode Theory of Wave Propagation*” Logos Press, 1961.
5. Wait, J. R., *Electromagnetic Waves in Stratified Media*, Pergamon, Taritown, N.Y., 1962.
6. Wait, J. R., “*Terrestrial Propagation VLF Waves, J. Res.*, NBS (National Bureau of Standards) 64D, (Radio Prop) ”1960 - 153.
7. SID Manual. “published from the Stanford Solar Center” – 20053
8. Raulin J.P., Bertoni F.C., Gavilan H.R. Samanes J.C., “Long-term and transient forcing of the low ionosphere monitored by SAVNET”, *PROPAGATION EFFECTS OF VERY LOW FREQUENCY RADIO WAVES*: Proceedings of the 1st International Conference on Science with Very Low Frequency Radio Waves: Theory and Observations. AIP Conference Proceedings, Volume 1286, pp. 3-41, DOI: [10.1063/1.3512893](https://doi.org/10.1063/1.3512893), 2010.]

9. Yokoyama, E., and, Tanimura, *Some long-distance transmission phenomena of Low frequency waves, Proc. IRE*, 21,263-270, 1933.
10. Crombie, D. D., Periodic fading mode of VLF signals received over long paths during sunrise and sunset, *J. Res. Natl. Bur. Stand., Sect. D*, 68, 27-34, 1964.



This pdf circulated in  
Vol. 4, Number 46,  
on 27 April 2012.